Phys. Scr. **T155** (2013) 014063 (7pp) doi:10.1088/0031-8949/2013/T155/014063

Measuring Lagrangian accelerations using an instrumented particle

R Zimmermann[1], L Fiabane[1], Y Gasteuil[2], R Volk[1] and J-F Pinton[1]

[1] Laboratoire de Physique, ENS de Lyon, UMR CNRS 5672, Université de Lyon, France
[2] smartINST S.A.S., 46 allée d'Italie, 69007 Lyon, France

E-mail: robert.zimmermann@ens-lyon.org

Received 7 June 2012
Accepted for publication 24 July 2012
Published 16 July 2013
Online at stacks.iop.org/PhysScr/T155/014063

Abstract
Accessing and characterizing a flow imposes a number of constraints on the employed measurement techniques; in particular, optical methods require transparent fluids and windows in the vessel. Whereas one can adapt the apparatus, fluid and methods in the laboratory to these constraints, this is hardly possible for industrial mixers. In this paper, we present a novel measurement technique which is suitable for opaque or granular flows: consider an instrumented particle, which continuously transmits the force/acceleration acting on it as it is advected in a flow. Its density is adjustable for a wide range of fluids and because of its small size and its wireless data transmission, the system can be used both in industrial and in scientific mixers, allowing for a better understanding of the flow within. We demonstrate the capabilities and precision of the particle by comparing its transmitted acceleration to alternative measurements, in particular in the case of a turbulent von Kármán flow. Our technique proves to be an efficient and fast tool to characterize flows.

PACS numbers: 47.27.−i, 47.51.+a, 47.80.−v

(Some figures may appear in color only in the online journal)

1. Introduction

Experimental fluid dynamics research in the laboratory consists of an interplay of suitable flow generation devices, working fluids, measurement techniques and analysis, with goals ranging from fundamental research in statistical/nonlinear physics to the optimization of mixers in industrial R&D departments. In this endeavor, very significant progress has been achieved during the last decade with the advent of space- and time-resolved optical techniques based on high-speed imaging [1]. However, direct imaging is not always possible, especially in industry: opaque vessels, non-transparent fluids, and environmental constraints, among others, may be limiting factors. Even when the fluid is transparent, the injection of tracer particles might still be not allowed or unsuitable, due to bio-medical or food regulations or due to the chemical properties of the fluid. While techniques using other kinds of probing waves (e.g. acoustics [2]) have been developed, a direct resolution of the Eulerian flow pattern is not always possible. In this context, Lagrangian techniques provide an interesting alternative, particularly for problems related to mixing [3, 4].

Lagrangian tracers with a temperature-sensitive dependence have been used in the study of Rayleigh–Bénard convection [5], a problem for which our group has developed *instrumented particles* [6–9]. The approach was to instrument a neutrally buoyant particle in such a way that it measures the temperature fluctuations during its motion as it is entrained by the flow, while transmitting the data via radio frequency to a laboratory operator in real time. Meaningful information regarding the statistics of thermion plumes has been obtained, showing excellent agreement with other techniques [5] and direct numerical simulations [10]. In the work reported here, we built upon this approach to instrument the particle such that one gets flow parameters directly from the measurements (in [6], one had to simultaneously film the particle motion). We equip the particle with a three-axis accelerometer, whose measurements are sampled at a rate equal to 316 Hz and transmitted to the laboratory operator. This particle is intended for turbulent flows. Thanks to its radio transmission it is suitable for opaque fluids or apparatuses without access for optical measurement techniques. Its continuous operation is also advantageous over particle tracking techniques that have to operate in chunks as the memory of the tracking

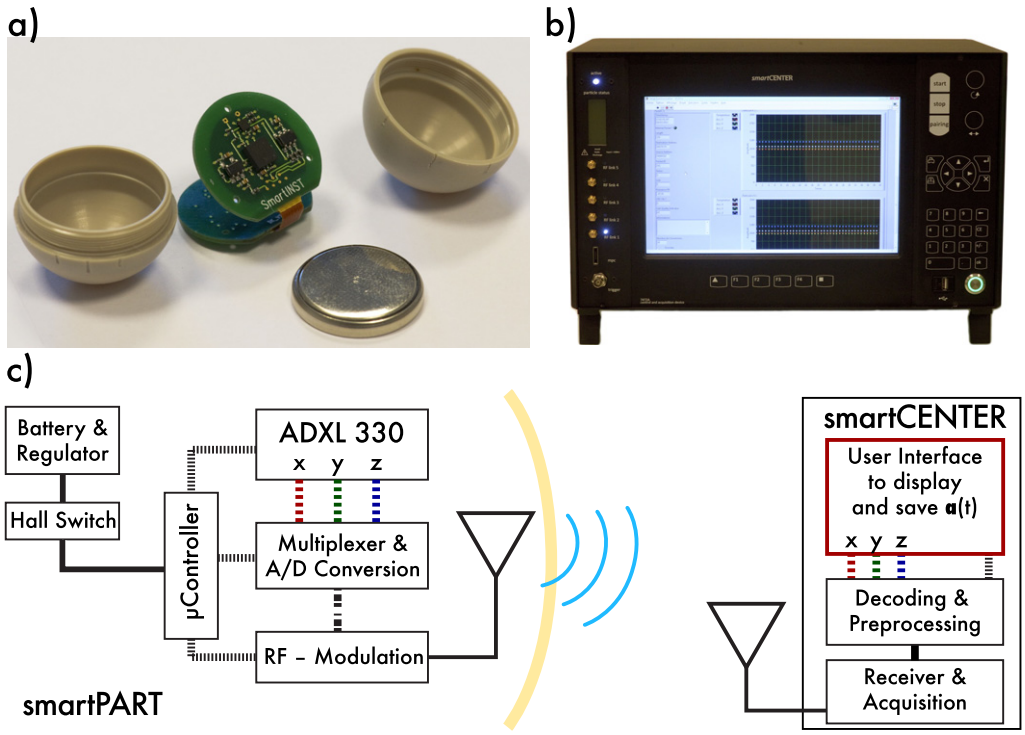

Figure 1. (a) and (b) The instrumented particle (*smartPART*) and its data control acquisition unit (*smartCENTER*). The coin cell is 20 mm in diameter. Cables and antenna are not shown here. The diagram in (c) sketches how the acceleration measurement is transmitted to and processed at the smartCENTER.

cameras is necessarily limited. Moreover and in contrast to tracer particles, this instrumented particle can be easily re-extracted from the apparatus after the experiment. However, as the particle is advected in a flow it rotates and consequently continuously changes its orientation with respect to the laboratory frame. Thereby the signals of the three-dimensional (3D) accelerometer are altered in a non-trivial way, and a detailed characterization and methods for extracting meaningful information from the acceleration signals are needed. We present here the preliminary results of a characterization.

This paper is organized as follows. First, we present the instrumented particle and additional techniques needed for its characterization (section 2). In section 3, we present an analysis of the results obtained in two different configurations: first, a simple pendulum with the particle attached at the end of a stiff arm, and then the particle advected in a fully turbulent flow. In order to verify that the transmitted acceleration is well related to its motion, we compare the results with simultaneous alternative measurements. Finally, we discuss the limitations and perspectives of this new measurement technique (section 4).

2. 'Smart particles'

The apparatus described in the following is designed and built by smartINST S.A.S., a young startup situated on the ENS de Lyon campus. The device consists of a spherical particle (the so-called smartPART) which embarks an autonomous circuit with a 3D-acceleration sensor, a coin cell and a wireless transmission system; and a data acquisition center (the so-called smartCENTER), which acquires, decodes, processes and stores the signal of the smartPART (see figure 1). The ensemble—smartPART and smartCENTER—measures, displays and stores the 3D acceleration vectors acting on the particle as it is advected in the flow. The accelerations are observed in a moving and rotating coordinate system and consist of four contributions: gravity, translation, noise and possibly a weak contribution of the rotation around the center of the particle itself.

2.1. Design and technical details

2.1.1. Sensor. The central component of the particle is the ADXL 330 (Analog Device)—a three-axis accelerometer. This component belongs to the category of micro-electro-mechanical systems (MEMS). Each of the three axes returns a voltage proportional to the force acting on a small, movably mounted mass-load suspended by micro-fabricated springs. The three axes of the ADXL 330 are decoupled and form an orthogonal coordinate system attached to the chip package. From this construction arises a permanent measurement of the gravitational force/acceleration $\boldsymbol{g} \equiv 9.8\,\mathrm{m\,s^{-2}} \cdot \hat{\boldsymbol{e}}_g = g \cdot \hat{\boldsymbol{e}}_g$. Each axis has a guaranteed minimum full-scale range of $\pm 3\,g$; however, we observe a typical range of $\pm 3.6\,g = 35\,\mathrm{m\,s^{-2}}$ per axis. The sensor has to be calibrated to compute the physical accelerations from the voltages of the accelerometer.

2.1.2. smartPART. The signals from the ADXL 330 are first-order low-pass filtered at $f_c = 160\,\mathrm{Hz}$ and then digitized at 12 bits and 316 Hz sampling rate. A multiplexer prior to the signal digitization induces a small time shift between the components of 0.64 ms. The output is then reshaped into

small packets and sent via radio frequency. The ensemble is powered by a coin cell. A voltage regulator ensures a stable supply voltage and thus a constant quality of the measurement. A Hall switch allows one to power-down most components; thereby, the battery is only used during experiments. Depending on the power needed to transmit the acceleration signals, a particle operates continuously for 6–36 h. The ADXL 330 is soldered to the printed circuit board such that it is situated close to the geometrical center of the particle. The particle itself is spherical with a diameter of 25 mm. The capsule walls are made of polyether–ether–ketone, which is known for its excellent mechanical and chemical robustness. It is leak-proof and its density can be matched to fluids by adding extra weight (namely tungsten paste) to the particle's interior; within the density range of 0.8–1.4 g cm^{-3} a relative density match of better than 10^{-4} is achievable. The particle is thus suited for most experiments in water and water-based solutions. It should be noted that the mass distribution inside the particle is neither homogeneous nor isotropic: in particular, its center of mass does not coincide with the geometrical center, making it out-of-balance. In practice, this results in a pendulum-like motion of the particle in the flow. Nevertheless, the imbalance can be adjusted to some extent by adding patches of tungsten paste to its interior, and the particles we use are carefully prepared such that they are neutrally buoyant, avoid any pendulum-like behavior and rotate easily in the flow.

2.1.3. smartCENTER. The signals from the smartPART are received by an antenna connected to the smartCENTER, which contains radio reception, processing and display units. It demodulates and decodes in real time the received raw signal into a time series of raw voltages of the ADXL 330. The physical acceleration sensed by the smartPART $\boldsymbol{a}_{\mathrm{SP}}$ can then be computed:

$$\boldsymbol{a}_{\mathrm{SP}} = \begin{pmatrix} a_1 \\ a_2 \\ a_3 \end{pmatrix} = \begin{pmatrix} (A_1 - O_1)/S_1 \\ (A_2 - O_2)/S_2 \\ (A_3 - O_3)/S_3 \end{pmatrix}, \tag{1}$$

where A_i, O_i and S_i are the measured raw signal, the offset and the sensitivity of each axis, respectively. Offset and sensitivity have to be calibrated beforehand; the procedure is described in the following section. The resulting time series are saved for further processing.

2.2. Calibration and robustness

The offset and sensitivity of the ADXL 330 have to be calibrated to convert the measured voltages into a physical acceleration. The axes of the accelerometer form an orthogonal coordinate system according to equation (1). At rest one observes only gravity projected onto the sensor at an arbitrary orientation. The observed raw values define consequently a translated ellipsoid (for simplicity we set $|\boldsymbol{g}| \equiv 1$):

$$\boldsymbol{a}_{\mathrm{SP}} \cdot \boldsymbol{a}_{\mathrm{SP}} = \sum_i \frac{(A_i - O_i)^2}{S_i^2} = \boldsymbol{g}^2 = 1. \tag{2}$$

Equation (2) can be arranged to

$$1 = \sum_i \left(\xi_i\, A_i^2 - 2\,\xi_{i+3}\, A_i\right), \tag{3}$$

with ξ_i six parameters containing offset and sensitivity. A sufficient number of measurements with different orientations define a set of equations which is solved using a linear least squares technique. Offset and sensitivity are then

$$O_i = \frac{\xi_{3+i}}{\xi_i} \quad \text{and} \quad S_i = \sqrt{\frac{1 + \sum_i \left(\xi_{3+i}^2/\xi_i\right)}{\xi_i}}. \tag{4}$$

We find that the particle at rest has an average noise of $\sigma_x = \sigma_y = 0.006\,g$ and $\sigma_z = 0.008\,g$, giving $|\boldsymbol{\sigma}| = \sqrt{\sum_i \sigma_i^2} = 0.012\,g$, where g is the magnitude of gravity. An analysis using the residuals showed a slightly higher resolution of $\sigma_x = \sigma_y = 0.005\,g$ and $\sigma_z = 0.003\,g$, and $|\boldsymbol{\sigma}| = 0.008\,g$. These values are thus the absolute errors of our measurement.

The ADXL 300 has among other things been chosen for its weak temperature dependence: its offset typically varies by 10^{-3} g °C^{-1}, and its sensitivity by 0.015 % °C^{-1}. Digitizing and transmission units were verified to be temperature independent. Consequently, the total temperature dependence of the smartPART is given by its accelerometer. For high-precision measurements, it is advised to calibrate the particle at experiment temperature shortly before the actual experiment.

We noted a small drift of the order of 0.005 g h^{-1} for the z-axis. No drift was observed for the x- and y-axis. Since a voltage regulator ensures a stable supply voltage of the circuit, this drift stems most likely from the internal construction of the accelerometer. Owing to the continuous data transmission of the instrumented particle, one flow configuration can be characterized in approximately 30 min. Hence, the little drift of the z-axis can be neglected.

Considering the mechanical robustness, the smartPART survived several days in a von Kármán mixer and neither contacts with the wall nor those with the sharp edged blades of the fast rotating propellers damaged its function or shell.

3. Acceleration signals

As mentioned before, the smartPART transmits in real time the accelerations acting on the particle as it is advected in the flow. The noise-to-signal ratio being small, we neglect the noise from here on. The contributions consist therefore of: gravity, translation and rotation of the particle. We now test the accuracy of the particle signals in two different experimental configurations by comparison with alternative measurements.

3.1. A two-dimensional (2D) pendulum

A pendulum is a simple and well-known case, ideal to measure the resolution of the particle. A stiff pendulum with a 60 cm long stiff arm is equipped with a position sensor returning the deflection angle φ of the arm. The particle is fixed at known length, l, with a known arbitrary orientation to the arm. The fact that a rotation of the particle around its center is restricted implies that the contribution

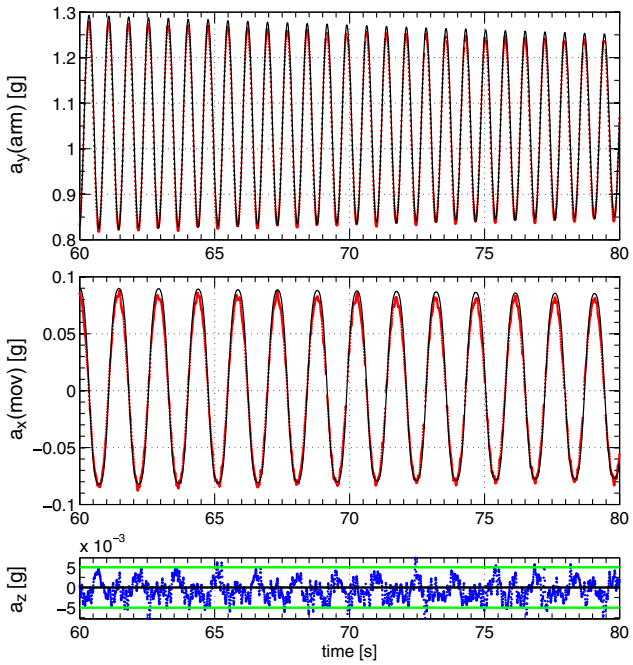

Figure 2. Comparison of the particle's signal $\boldsymbol{a}_{\mathrm{SP}}(t)$ (•) to the theoretical curves based on the position sensor (—). a_y points with the arm and a_x measures the force in the direction of the movement. No force is exerted along the z-axis (the green lines represent the uncertainty of the calibration). Note that acceleration is measured in $g = 9.8\,\mathrm{m\,s^{-2}}$.

from the rotation of the particle around its center is known. Measuring $\boldsymbol{a}_{\mathrm{SP}}$ at rest ($\varphi = 0^\circ$) and at several arbitrary positions, one can determine the axis of rotation of the arm. Once this vector is known the measured acceleration signal is rotated/re-expressed such that a_y points with the arm, a_x with the movement and a_z with the axis of rotation. Note that by definition the latter does not change when the pendulum moves. The signal seen by the particle is a 2D problem and is fully described as a function of the deflection angle φ:

$$\begin{aligned} a_x(\varphi) &= g\ \sin\varphi + l\,\ddot{\varphi}, \\ a_y(\varphi) &= g\ \cos\varphi + l\,\dot{\varphi}^2. \end{aligned} \tag{5}$$

In the limit of the small angle approximation, this simplifies to the well-known oscillations of frequency ω:

$$\begin{aligned} a_x(\varphi) &\approx -l\omega^2\ \sin\omega t, \\ a_y(\varphi) &\approx g + \frac{l\,\omega^2}{2}(1+\cos 2\omega t). \end{aligned} \tag{6}$$

The simultaneous measurement of the angle, $\varphi(t)$, and the particle's signal, $\boldsymbol{a}_{\mathrm{SP}}(t)$, enables us to compare the two signals without any other approximation or fit than equation (5).

Figure 2 shows $\boldsymbol{a}_{\mathrm{SP}}(t)$ for several periods of the pendulum, measured by the smartPART and by the position sensor. The agreement between the two signals is very good, and in particular better than the uncertainty of the calibration. Hence, the Lagrangian acceleration of the smartPART corresponds well to its actual motion in this simple case. We now move on to more complicated motions.

3.2. Fully developed (3D) turbulence

The instrumented particle is intended for the characterization of complex/turbulent flows. Such flows exhibit strong, intermittent variations in the acceleration. To verify the suitability of the smartPART for these conditions, we now investigate its motion in a fully turbulent mixer while tracking it with an independent optical technique.

Namely, we use a von Kármán water flow: a swirling flow is created in a square tank by two opposing counter-rotating impellers of radius $R = 9.5\,\mathrm{cm}$ fitted with straight blades 1 cm in height. The flow domain in between the impellers has characteristic length $H = 20\,\mathrm{cm} \cong 2R$ (see figure 3) and the vessel is built with transparent flat side walls, allowing direct optical measurements over almost the whole flow domain. Blades on the impellers work similarly to a centrifugal pump and add a poloidal circulation at each impeller. For counter-rotating impellers, this type of flow is known to exhibit fully developed turbulence [11]. Within a small region in the center the mean flow is little and the local characteristics approximate homogeneous turbulence. However, at a large scale it is known to have a large-scale anisotropy [12, 13]. At a propeller frequency of 3 Hz, we estimate a Reynolds number based on the Taylor micro-scale of $R_\lambda = 500 \pm 50$.

We optically track the translation and absolute orientation of the smartPART while simultaneously acquiring the transmitted acceleration time series. These optical measurements are then used as a reference to compare with the instrumented particle's signals. The six-dimensional tracking technique (or 6D tracking, three components for the translation and three components for the rotation of the particle around its center) is explained in detail in [14, 15] and briefly sketched here (figure 3). In order to determine the absolute orientation, the particle is textured by hand using a black-ink permanent marker (see figure 3(c)). Acceleration sensor and texture are then calibrated/retrieved independently; nevertheless, the accelerometer is at a fixed but unknown orientation with respect to this texture, i.e. the sensor and texture are related by a constant rotation matrix. We determine this matrix by acquiring the acceleration signals of the particle at arbitrary orientations while additionally determining its orientation and the location of gravity on the texture. The particle is then inserted into the apparatus, which is illuminated by high-power LEDs. Its motion is tracked by two high-speed video cameras (Phantom V12, Vision Research), which record synchronously two views at approximately 90°. The observation volume is $15 \times 15 \times 15\,\mathrm{cm}^3$ in size and resolved at a resolution of $4.2\,\mathrm{pixel\,mm^{-1}}$. In our configuration, a camera can store of the order of 14 000 frames in on-board memory, thus limiting the duration of continuous tracks. Therefore, a computer issues the recording of 8 bit gray-scale movies at a sufficiently high frame rate while controlling the smartCENTER such that the acceleration signal and images are synchronized. After extracting the time series of the particle's position and orientation, one can then compare the accelerometer's signal to the motion of the particle.

It should be stressed that the two measurement techniques observe the motion of the instrumented particle in two completely different reference frames. On the one hand, the 6D tracking uses a fixed, non-rotating coordinate system, and

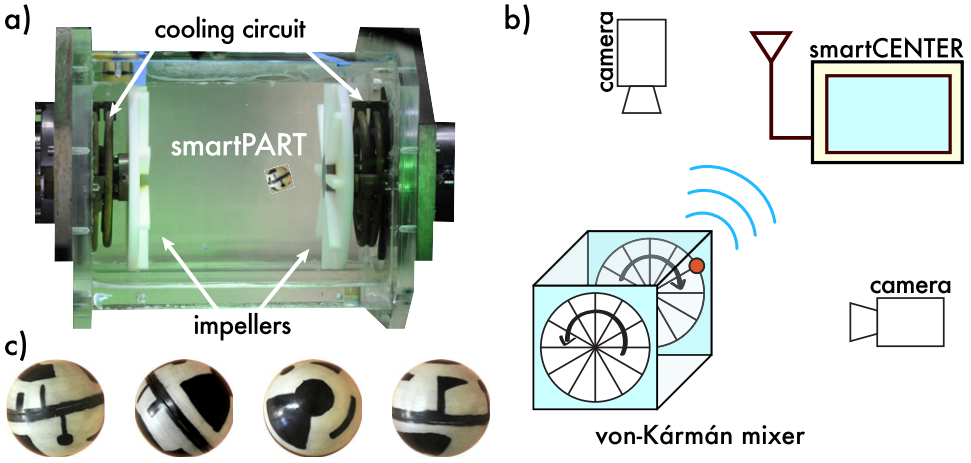

Figure 3. Experimental setup: (a) a picture of the apparatus; (b) a sketch of the arrangement; and (c) a textured instrumented particle at different orientations.

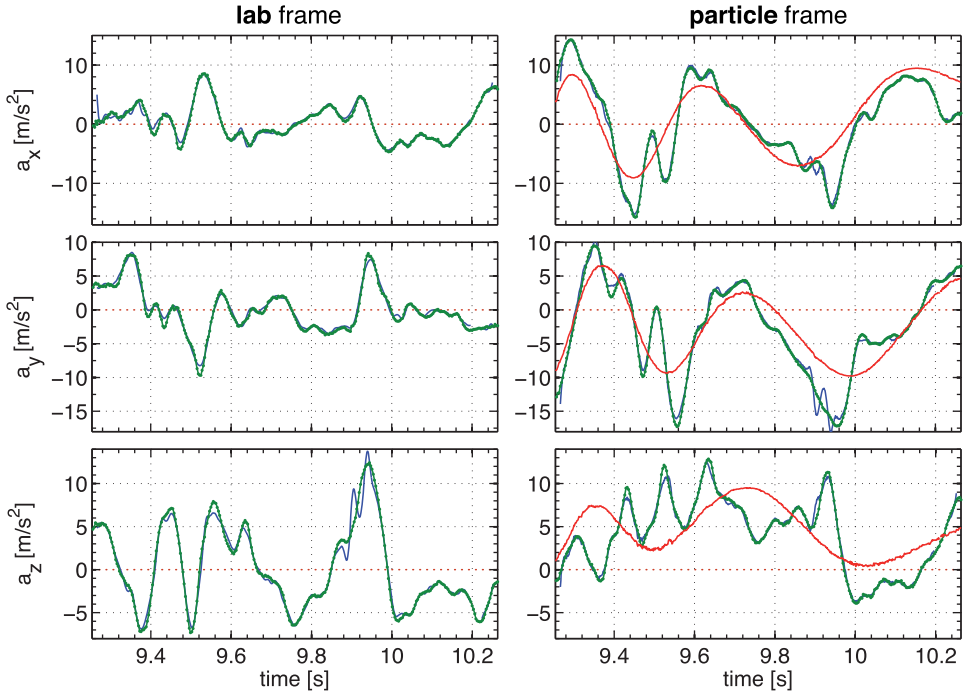

Figure 4. A sample trajectory of the instrumented particle seen by the camera (—) or smartPART (•); it is $f_{\text{prop}} = 3$ Hz. The absolute orientation enables us to re-express the camera measurement of the particle (laboratory frame) in the moving frame of the particle and vice versa. In the former, gravity is subtracted and in the particle frame gravity is represented by the red line.

is referred to as the laboratory frame. On the other hand, as the particle is advected and turned in the flow, it and consequently the embarked accelerometer constantly rotate their coordinate system with respect to the laboratory frame; the acceleration signal is thus measured in a frame which is continuously rotating and not fixed. This frame is referred to as the particle frame. The acceleration sensor measures the forces acting on it as it moves in the flow. Knowing the absolute orientation of the particle at each instant we can express the signal of the smartPART in the laboratory frame by rotating it such that it corresponds to a non-rotating particle. Starting from the time series of position and orientation, it is also possible to compute the linear, centrifugal and gravitational acceleration/force acting on a point inside the particle and then project these into the rotating particle frame. The different components are then expressed in the frame of the sensor.

Figure 4 shows a sample trajectory in both coordinate systems. The agreement between the two techniques is remarkable. Furthermore, one observes that the projection of gravity is continuously changing: the particle is rotating in a non-trivial way. Deviations between the two techniques stem from several experimental errors. Firstly, the position measurement: bubbles, reflections and other impurities alter the measured position of the particle. The acceleration is the second derivate and thus highly sensitive to such events. Secondly, the orientation measurement: the absolute orientation is needed to change between the reference frames. The uncertainty in the absolute orientation is typically 3°;

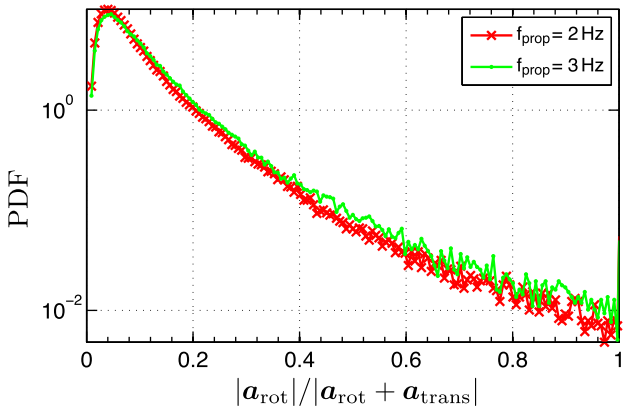

Figure 5. Ratio of the rotational forces to the total force acting on the particle. The 80th percentile is found at a ratio of 0.14 and 0.16, respectively.

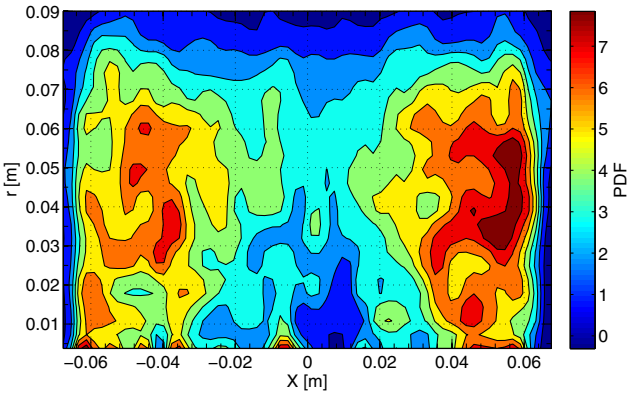

Figure 6. Preferred position of the instrumented particle: independent of the propeller speed it is mostly situated in a torus shape around the propeller.

that results in a wrong projection of gravity of $\pm 0.5\,\mathrm{m\,s^{-2}}$. It further biases the rotational forces, as they are derivatives of the orientation time series. Finally, the matrix relating the sensor and texture: this matrix is constant and thus a systematic contribution. The uncertainty is less than 2°—i.e. the error in projecting gravity is $<0.3\,\mathrm{m\,s^{-2}}$. The observed agreement in the laboratory frame, $\Delta\boldsymbol{a} = \boldsymbol{a}_{\mathrm{SP}} - \boldsymbol{a}_{\mathrm{6D}}$, between the two techniques is as follows: all three components of $\Delta\boldsymbol{a}$ have the same probability density function (PDF). Surprisingly, the (absolute) uncertainty almost doubles by increasing f_{prop} from 2 to 3 Hz. Nevertheless, for 80% of the data the agreement is better than 0.8 and $1.6\,\mathrm{m\,s^{-2}}$, respectively. For comparison, the absolute value $|\boldsymbol{a}_{\mathrm{6D}}|$ has a mean of 2.9 and $6.6\,\mathrm{m\,s^{-2}}$ and a standard deviation of 1.8 and $4.1\,\mathrm{m\,s^{-2}}$, respectively. The signal of the particle thus corresponds to the flow; however, its interpretation is not simple. In particular, and after comparing many different trajectories, it becomes clear that no easy transformation is available to get rid of the rotation of the particle.

By construction the center of the accelerometer is placed at $\boldsymbol{r} = 3\,\mathrm{mm} \cdot \hat{\boldsymbol{e}}_z$. A rotation of the particle around its geometric center will thus add a centrifugal contribution to the measured acceleration. This raises the question of which term—translation or rotation of the particle—dominates the acceleration signal. To address this question, we take advantage of the 6D tracking, which enables us to compute the different forces acting on a point at $\boldsymbol{r} = 3\,\mathrm{mm} \cdot \hat{\boldsymbol{e}}_z$ inside the sphere. We can thus compare the contribution of the translation and that of the rotation of the particle. Figure 5 shows the ratio of the rotational (i.e. centrifugal) acceleration, $\boldsymbol{a}_{\mathrm{rot}} = \boldsymbol{\omega} \times \boldsymbol{\omega} \times \boldsymbol{r} + \frac{\mathrm{d}\boldsymbol{\omega}}{\mathrm{d}(t)} \times \boldsymbol{r}$, to the total acceleration, $\boldsymbol{a}_{\mathrm{trans}} + \boldsymbol{a}_{\mathrm{rot}}$ (without gravity). Dimensional arguments tell us that $a_{\mathrm{trans}} \propto f_{\mathrm{prop}}^2$ and $a_{\mathrm{rot}} \propto f_{\mathrm{prop}}^2$. Consistently, the PDF of the ratio $|\boldsymbol{a}_{\mathrm{rot}}|/|\boldsymbol{a}_{\mathrm{trans}} + \boldsymbol{a}_{\mathrm{rot}}|$ differs only a little for the two propeller frequencies. Moreover, it is peaked at 5% and the 80th percentile is at a ratio of 14 and 16%, respectively. Hence, it is legitimate to neglect the rotational forces if no 6D tracking is available.

4. Discussion

In the latter part of this paper, we studied the behavior of a large neutrally buoyant sphere in a turbulent flow. Comparing with solid spheres of the same size in the same mixer, we find that the particle, in general, behaves almost identically [16]. In particular (and despite the fact that the instrumented particle is neutrally buoyant), we observe that it generally stays in a region close to the impellers. Figure 6 shows the PDF of position for the smartPART. Independent of the impeller speed, it is mostly situated in a torus shape around the propeller, exhibiting a preferential sampling of the flow for these large neutrally buoyant spheres.

Moreover, since we investigate large particles with a size D_{part} comparable to the integral length scale, L_{int}, moving through the whole mixer, the Kolmogorov assumptions to characterize turbulence are no longer valid. For these reasons, the smartPART can be insufficient to access all the details of a turbulent flow: some parts of the flow are hardly explored, and some scales of the turbulence might be filtered due to the size of the instrumented particle. However, one should bear in mind that these features of the flow are often accessed by means of optical methods, whereas the instrumented particle operates also in environments and fluids that are unsuitable for optical measurement techniques.

Some other experimental constraints should be additionally stressed here. As already mentioned, the mass distribution inside the particle is neither homogeneous nor isotropic. It is therefore possible that the particle is out of balance, i.e. that the center of mass does not coincide with the geometrical center. Such a particle has a strong preferred orientation and wobbles similarly to a kicked physical pendulum. The imbalance can be adjusted to some extent by adding weight to its interior, but the particle must be prepared very carefully and one must make sure that the particle used is well balanced and rotates easily in the flow.

Also, the receiver/demodulation unit of the smartCENTER works best within a range of radio power, i.e. particles that are emitting either too strongly or too weakly are undesirable and one has to adjust the radio emission of the smartPART. A stronger radio emission power can be required, e.g. if the apparatus builds a Faraday cage (i.e. an electrically connected metal structure surrounds the flow), or if the signal has to pass a longer distance in more water or in a bigger apparatus. Solutions with a high conductivity are also likely to damp the radio signal. Naturally, a stronger radio emission shortens the lifetime of the battery. Nevertheless,

particles with stronger radio emission still last 6–12 h, which is sufficient in most cases.

To conclude, we have presented the working principle of an instrumented particle giving a measure of the three components of the Lagrangian acceleration. We were able to show that the Lagrangian acceleration of the smartPART corresponds well to its actual translation and is not biased by a possible rotation of the particle around its center. Work on extracting detailed information on the flow from the acceleration time series is ongoing. These instrumented particles can shed some light on mixers which were not or hardly accessible up to now. Due to its continuous transmission, one flow configuration can be characterized within ∼30 min. Apart from its appeal to the chemical and pharmaceutical industries, it might be an interesting tool for quantifying flows in laboratories.

Acknowledgments

This work was partially supported by ANR-07-BLAN-0155. The authors acknowledge the technical help of Marius Tanase and Arnaud Rabilloud for the electronics, and of all of the ENS machine shop team. The authors also thank Michel Voßkuhle, Mickaël Bourgoin and Alain Pumir for fruitful discussions. Finally, RZ warmly thanks the TMB-2011 committee for granting a 'Young Scientist Award' of the 2011 Turbulence Mixing and Beyond conference for the work presented in this paper.

References

[1] Tropea C, Yarin A and Foss J F (ed) 2007 *Springer Handbook of Experimental Fluid Dynamics* (Berlin: Springer)
[2] Mordant N, Metz P, Michel O and Pinton J-F 2001 *Phys. Rev. Lett.* **87** 214501
[3] Toschi F and Bodenschatz E 2009 *Annu. Rev. Fluid Mech.* **41** 375
[4] Shraiman B and Siggia E 2000 *Nature* **405** 639
[5] Ni R, Huang S-D and Xia K-Q 2012 *J. Fluid Mech.* **692** 395
[6] Gasteuil Y, Shew W L, Gibert M, Chillà F, Castaing B and Pinton J-F 2007 *Phys. Rev. Lett.* **99** 234302
[7] Gasteuil Y 2009 *PhD Thesis* École Normale Supérieure de Lyon, Lyon
[8] Shew W L, Gasteuil Y, Gibert M, Metz P and Pinton J-F 2007 *Rev. Sci. Instrum.* **78** 065105
[9] Pinton J-F, Metz P, Gasteuil Y and Shew W L 2009 Mixer and device and method for monitoring or controlling said mixer *Patent US* 2011/0004344 A1
[10] Schumacher J 2009 *Phys. Rev.* E **79** 056301
[11] Ravelet F, Chiffaudel A and Daviaud F 2008 *J. Fluid Mech. Digit. Arch.* **601** 339
[12] Ouellette N T, Xu H, Bourgoin M and Bodenschatz E 2006 *New J. Phys.* **8** 102
[13] Monchaux R, Ravelet F, Dubrulle B, Chiffaudel A and Daviaud F 2006 *Phys. Rev. Lett.* **96** 124502
[14] Zimmermann R, Gasteuil Y, Bourgoin M, Volk R, Pumir A and Pinton J-F 2011 *Rev. Sci. Instrum.* **82** 033906
[15] Zimmermann R, Gasteuil Y, Bourgoin M, Volk R, Pumir A and Pinton J-F 2011 *Phys. Rev. Lett.* **106** 154501
[16] Zimmermann R 2012 *PhD Thesis* École Normale Supérieure de Lyon, Lyon